Astron. Astrophys. 318, 187–197 (1997)

ASTRONOMY
AND
ASTROPHYSICS

Circularization and synchronization times in Main-Sequence of detached eclipsing binaries

II. Using the formalisms by Zahn

A. Claret[1] **and N.C.S. Cunha**[2]

[1] Instituto de Astrofísica de Andalucía, CSIC, Apartado 3004, E-18080 Granada, Spain
[2] Laboratorio de Astrofísica Espacial y Física Fundamental, INTA, Apartado 50727, E-28080 Madrid, Spain

Received 27 November 1995 / Accepted 2 July 1996

Abstract. Double-lined eclipsing binaries with accurate absolute dimensions are the best stellar data to test tidal evolution theories due to the high dependency of the time scales on masses, relative radii and periods. In a preceding paper we have probed the hydrodynamical mechanism against the observed levels of synchronization and circularization for about 40 close binary systems with accurate absolute dimensions. In the present work we extend our investigations, using the same systems as a control, to the turbulent dissipation and radiative damping mechanisms which have been studied by Zahn. The time scales for these processes are characterized by the parameters λ_2 and E_2 respectively. These parameters were computed for a wide grid of stellar models and they are presented, for the first time, as functions of the mass and time.

The differential equations which govern the orbital parameters were integrated using our recent grids of stellar models (Claret 1995,1996 ; Claret & Giménez 1995). The derived critical times and radii were compared with observations of synchronization and circularization levels. Within uncertainties, the formalisms by Zahn seem to be able to explain the eccentricity distribution around the zero point of the diagram log (age/t_{cri}) $\times$ eccentricity although they can not explain some systems with circular orbits which present ages smaller than their respective critical times.

We have also introduced a diagram based on the integration of the differential equations which proved to be useful to test theoretical predictions for the relationship age $\times$ Period (cut-off) for clusters. Using this diagram we have shown that the turbulent friction mechanism is not dissipative enough to explain such an observational relationship. However, as these results are valid only for little departure from synchronism and small eccentricity, we plan to investigate the influence of the initial conditions in a forthcoming paper.

Key words: stars: binaries: close; evolution; rotation

Send offprint requests to: A. Claret (claret@iaa.es)

1. Introduction

During the most recent years the interest in the tidal evolution theory has been revived. The impact of the better quality of observations in close binary systems was of capital importance to increase such interest because theoretical predictions could be compared with them and improved, if required. Observations of close binaries in clusters were also important because they gave information on the circularization levels for these coeval samples. To get direct information on masses and radii for these close binaries is not a simple task but these observations are useful to obtain the so-called cut-off period (Mayor & Mermilliod 1984). As its name indicates, this is the period that characterizes the transition between circular and eccentric orbits. A relationship between the age of the cluster and the cut-off period was found by Mathieu et al. (1992). Comparison between these critical periods and those derived from the different mechanisms of circularization is also an excellent tool to test tidal theory.

From the theoretical point of view three mechanisms have been used to investigate the orbital evolution of close binary systems. The first braking mechanism is mainly based on the work of Tassoul (1987, 1988). Following this description, the stars in a close binary system tend to synchronize and circularize the orbit due to the distortions which cause large scale hydrodynamical currents. In this description the time scale for circularization is proportional to $P^{49/12}$ where P is the period. Another characteristic of Tassoul formalism is that the time scales for synchronization (TSS) and circularization (TSC) depend on a free parameter N in such a way that $10^N = \nu_t/\nu_r = R$ where ν_t is the eddy viscosity in the external zone, ν_r is the radiative viscosity (including the plasma one) and R is the Reynolds number. As the equations were derived under the assumption of little depart from asynchronysm and other approaches- the spin-down time acts only as a lower limit - Tassoul introduced in the hydrodynamical TSS and TSC an adjustable parameter γ which takes into account these limitations.

The hydrodynamical mechanism can be applied to stars with radiative cores and convective envelopes as well as to massive stars: for the former case N is of the order of 10 while for the latter N is around 0. In a recent paper we have investigated this mechanism using homogeneous data for eclipsing binaries with accurate absolute dimensions as a control (Claret et al. 1995, Paper I). In that paper we have introduced a correction on the TSC which takes into account the contribution of both components. Note that such a correction should be considered in spite of the tidal theory used.

Rieutord 1992 has some reservations on the hydrodynamical mechanism. He has argued that the"large-scale flows driven by Ekman pumping in the spin-up/down of a tidally distorted star is not efficient enough to reduce the synchronization time". If stars are made of an incompressible viscous fluid, the synchronization time is of the order of the viscous time. In a more recent paper by Tassoul & Tassoul 1996 this argument was refuted. We return to this subject below.

On the other hand, Zahn (1966, 1970, 1975, 1977, 1989) investigated the effects of turbulent dissipation and radiative damping on the synchronization and circularization of binary systems. Both mechanisms are responsible for the tidal friction on late-type and early-type stars respectively. According to Zahn a star in a binary system is subject to the gravitational field of its mate, and from this interaction a tidal bulge appears. If one assumes that the stars are synchronized this bulge is aligned but if there is depart from synchronism a delay in this perturbed region gives rise to a torque. This torque tends to bring the star back into to the synchronism.

In this paper we study the validity of both mechanisms by Zahn by comparing with observations. A procedure similar to that used in Paper I is followed. In section 2 we briefly describe the theoretical basis of the physical processes of tidal friction, the evolutionary models, the computational methods used to derive the coefficients involved with TSS and TSC, and the integration of the corresponding differential equations. Section 3 will be devoted to analysing the synchronism while section 4 deals with circularization. Finally, in section 5 we present our conclusions.

2. A brief description of the braking mechanisms and the evolutionary models

2.1. The braking mechanisms

Zahn 1992 and Tassoul & Tassoul 1996 reviewed the main aspects and advances in tidal evolution theory. We refer readers to these two papers for details. In this section we shall restrict our attention to the work developed by Zahn. Stars in a binary system react to the disturbing potential due the presence of the their mates through the equilibrium and dynamic tides. Tide equilibrium is retarded by the action of turbulent viscosity (Reynolds number can reach 10^{12}) and this process is very efficient for stars with deep convective envelopes. The turbulent dissipation is carried out in a time scale of the order of R^2/ν_t and Zahn (1966) has shown that the convective friction time t_f is given by

$$t_f = \left[\frac{MR^2}{L}\right]^{1/3} \tag{1}$$

where M is the stellar mass, R the radius and L the luminosity.

The TSS and TSC are given by (e.g. Zahn 1984)

$$\frac{1}{\tau_{sync}} = \frac{6k_2}{t_f} q^2 \frac{MR^2}{I}\left(\frac{R}{A}\right)^6 \tag{2}$$

$$\frac{1}{\tau_{cir}} = \frac{21k_2}{t_f} q(q+1)\left(\frac{R}{A}\right)^8. \tag{3}$$

In Eqs. 2 and 3 k_2 is the apsidal motion constant, which gives a measure of the mass concentration of stars, q is the mass ratio, I the momentum of inertia, and A is the semi major axis of the orbit. As the TSC is more dependent on the relative radii we would expect that stars should synchronize before circularizing the orbits. However, there are some prominent counter-examples as in the cases of TZ Fornacis (Claret & Giménez 1995a, this paper) and Capella (Claret 1995c). Here τ_{cir} and τ_{sync} denote the time scales. The critical times for circularization and synchronization derived from the integration of the corresponding differential equations will be represented by t_{cri} . This symbol will be applied to both cases since the context in which they will be quoted will avoid any problem of identification. The same holds for the critical surface gravity log g_{cri}.

For stars with convective core and radiative envelope the dissipation mechanism is due to radiative damping. The so-called g-modes can resonate with the periodic tidal potential in a binary system. If there is a departure from synchronysm the gravity waves produced by the convective core will be damped in the surface zone since the dissipation time is shorter than the tidal period. Following Zahn, "when some dissipative process is at work, a torque is applied to the star, due to the fact that the mass configuration was no longer the same symmetry properties as the total potential". Using an asymptotic approach to calculate the amplitude of the dynamic tide, we can obtain the corresponding TSS and TSC (Zahn 1975)

$$\frac{1}{\tau_{sync}} = 5\left(\frac{GM}{R^3}\right)^{1/2} q^2(1+q)^{5/6} E_2 \frac{MR^2}{I}\left(\frac{R}{A}\right)^{17/2} \tag{4}$$

$$\frac{1}{\tau_{circ}} = \frac{21}{2}\left(\frac{GM}{R^3}\right)^{1/2} q(1+q)^{11/6} E_2\left(\frac{R}{A}\right)^{21/2} \tag{5}$$

where E_2 is related with the dynamic tidal contribution to the total perturbed potential (see subsection 2.3). E_2 is similar to k_2 but it is much more dependent on the stellar structure than the apsidal motion constant.

2.2. Stellar models

We have used, for comparison with observational data, the stellar models by Claret 1995a,b and Claret & Giménez 1995b. The input physics can be summarized as

1. Mass loss rate during the main-sequence was included following Nieuwenhuijzen & de Jager 1990.
2. For the red giant phase, we have adopted the results by Reimers 1977.
3. Convection has been treated using the mixing length theory and the adopted α was 1.52 derived from the solar model calibration and compatible with the best binary stellar data available.
4. For models with convective cores, we considered overshooting given by α_{ov} = d/H$_p$ = 0.20.
5. The new radiative opacities with spin-orbit coupling (Iglesias et al. 1992) were used throughout except for temperatures lower than 6000 K and greater than 1-5$\times 10^8$ K. For these cases, we have used the tables provided by Alexander (1992) and the computations from Los Alamos (Huebner et al. 1977), respectively.
6. The nuclear network uses the CNO cycle, the three pp-chains and for the helium burning we adopted the reactions ^{4}He$(\alpha,\gamma)^8$Be$(\alpha,\gamma)^{12}$C(α,γ) ^{16}O$(\alpha,\gamma)^{20}$Ne.
7. The equation of state takes into account partial ionization through Saha's approximation, the pressure of gas and radiation as well as the equations for degenerate electrons. For less massive models alternative equations of state can be used (see Claret 1995a).

The adopted chemical composition was (Y,Z)=(0.28,0.02) although for some specific cases models with different metallicities were used. If the stars of a given system are in a conflictive position on the HR diagram we have computed models for the observed masses in order to avoid problems with interpolations among the tracks, as for example DI Her, a system with very young components. In the following subsections we shall describe the computational methods used to derive the key coefficients needed to evaluate the time scales.

2.3. The calculation of the torque constants E_n

For stars with convective cores the time scale for circularization and synchronization depends on the parameter E$_n$, as we have seen before. That parameter is computed numerically given the complexity of the differential equations which must be solved. The general relationship between E$_n$ and the internal properties of the models is given by

$$E_n = \frac{3^{8/3}\left(\Gamma(4/3)\right)^2}{(2n+1)\,[n(n+1)]^{4/3}}\frac{\rho_f R^3}{M}\left[\frac{R}{g_s}\left(\frac{-gB}{x^2}\right)'_f\right]^{-1/3} H_n^2 \quad (6)$$

where Γ is the usual gamma function , x is normalized radius of the configuration, the symbol f denotes the border of the convective core, s indicates the surface, the prime denotes the derivative with respect to x, R is the radius, M the mass, g the gravity and B is given by

$$B = \frac{d}{dr}ln\rho - \frac{1}{\Gamma_1}\frac{d}{dr}lnP \quad (7).$$

This function B, which is positive in the convective core and negative in radiative regions, in fact gives the difference between the density gradient and that calculated adiabatically. Readers shall recognize that B is related with the Brunt-Väisälä frequency. In Eq. 7 Γ_1 is given by (dlnP/dlnρ)$_{adi}$.

The coefficient H$_n$ is an integral

$$H_n = \frac{1}{X(x_f)Y(1)}\int_0^{x_f}\left[Y'' - \frac{n(n+1)Y}{x^2}\right]X\,dx \quad (8)$$

where X is the solution of the differential equation

$$X'' - \frac{\rho'}{\rho}X' - \frac{n(n+1)}{x^2}X = 0 \quad (9)$$

and Y is the solution of Clairault equation written in a slightly different way, say

$$Y'' - 6\left(1-\frac{\rho}{\overline{\rho}}\right)\frac{Y'}{x} - \left[n(n+1) - 12\left(1-\frac{\rho}{\overline{\rho}}\right)\right]\frac{Y}{x^2} = 0 \quad (10)$$

.

In the last two equations ρ and $\overline{\rho}$ indicate the local and mean density at the distance r from the center. More detailed information on the above equations can be found in Kopal 1989 and Zahn (1970, 1975). In this paper we shall consider the case n=2.

As expected, the behaviour of the tidal constant E$_2$ is strongly dependent upon mass and time. For a given mass, E$_2$ is a strongly decreasing function of the convective core size. Thus, when the star evolves off the main-sequence its core shrinks and E$_2$ decreases very quickly. Hereafter, given that E$_2$ changes in several decades during stellar evolution for a given mass, we shall use the logarithmic scale. To illustrate the mass dependence Fig. 1 displays the value of log E$_2$ for several stellar masses near the ZAMS. For nearly homogeneous models of 1.6 and 32 M$_\odot$ log E$_2$ changes from -8.2 to -5.4. In the same figure the high dependence of E$_2$ on the size of the convective core can be seen for models near the ZAMS. In Fig. 2 we can see how log E$_2$ depends on time for a 15.8 M$_\odot$ stellar model with core overshooting (α_{ov}=0.20). When the convective core is very small log E$_2$ drops to -11. As already pointed out by Zahn (1977) we confirm that the coefficient E$_2$ is much more sensitive to the stellar structure changes than the apsidal motion k$_2$.

2.4. Tidal coefficient for stars with convective envelopes

For more massive stars with convective cores the time scales depend on the coefficient E$_2$ while their counter-parts are dependent on the coefficient λ_2. This coefficient, on the other hand, is connected with the structure of the external layers of the model. The apsidal motion constant k$_2$ was used as a first approach for

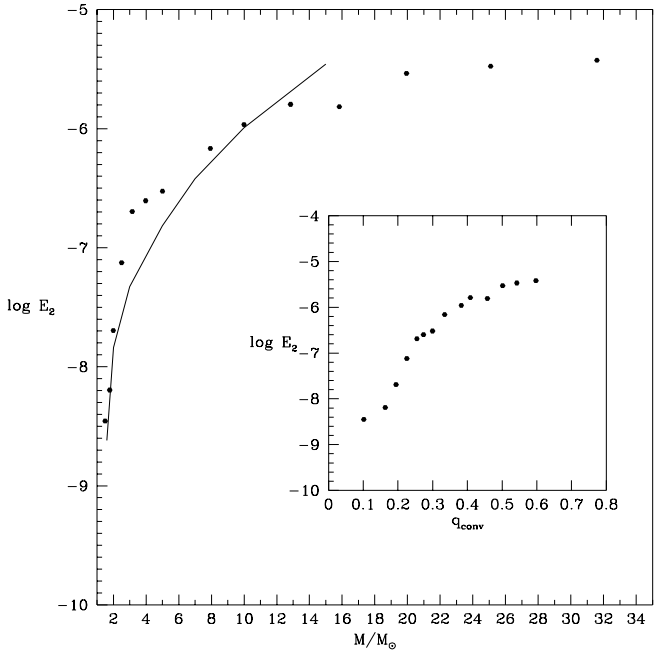

Fig. 1. The tidal constant E_2 as function of the mass near the ZAMS. The computations were done for X=0.70 and Z=0.02. Note that we have used a logarithmic scale. The calculations by Zahn (1975) for the ZAMS are shown for comparison (solid line). The lower right corner shows the dependence of E_2 on the size of the convective core.

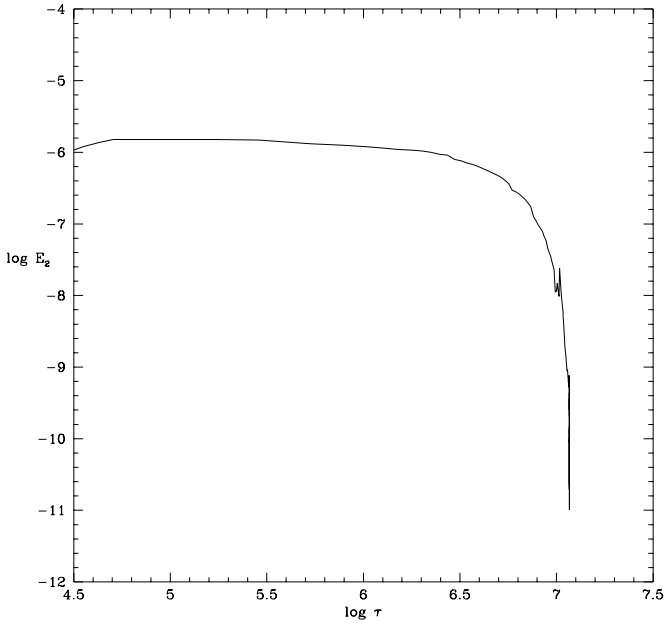

Fig. 2. Variation with time of log E_2 for a 15.8 $M_\odot$ model with core overshooting. Between the ZAMS and the point where the convective core disappears there is a variation of almost 5 dex.

λ_2 (Zahn 1977, 1984). In 1989 Zahn revised the theory of equilibrium tide using the mixing length theory as support. Now, we shall summarize his main results.

When the convective turnover time is small as compared with the tidal period we have

$$\lambda_2 = 0.607\alpha^{4/3}E^{2/3}\int_{xb}^{1} x^{22/3}(1-x)^2dx \qquad (11)$$

where x_b denotes the bottom of the surface convective zone, α is the mixing-length parameter and E describes a polytropic envelope. This variable was evaluated for each stellar configuration using

$$E = \frac{Q_{conv}}{\int_{x_b}^{1}\left(\frac{2(1-x)}{5x}\right)^{3/2}x^2dx} \qquad (12)$$

where Q_{conv} is the mass of the convective envelope.

Due to a reduction of the viscosity (see Zahn 1989, sec. 3) Eq. 11 should be modified to

$$\lambda_2 = 0.607\alpha^{4/3}E^{2/3}$$
$$\left[\int_{x_a}^{1} x^{22/3}(1-x)^2dx + x_a^{7/6}(1-x_a)^{3/2}\int_{x_b}^{x_a} x^{37/6}(1-x)^{1/2}dx\right] \qquad (13)$$

where

$${x_a}^{7/6}(1-x_a)^{3/2} = 1.198\left(\frac{5}{2}\right)^{3/2}\alpha^{-2/3}E^{-1/3}\frac{\Pi}{2t_f} \qquad (14).$$

In the last equation Π indicates the tidal period and t_f is the convective friction time.

In Fig. 3 we show the comparison between λ_2, computed using Eq. 11, and k_2 for 1.0 $M_\odot$ model during the main-sequence. As the model evolves the differences decrease and are always smaller than one order of magnitude. Similar behaviour occurs for models with similar masses. Note that the more the model is evolved, i.e., the more the convective envelope becomes deeper, the more k_2 tends to λ_2. Taking this general feature into account we can consider that apsidal motion is a good approximation, at least for a preliminary analysis.

2.5. Integration of the differential equations and a theoretical approach to the age × Period (cut-off) for clusters

At this point all variables needed to compute the TSC and TSS are known. However, in order to take into account the improvements introduced by Zahn 1989 in the theory of equilibrium tide, Eqs. 2 and 3 should be changed. Moreover, Eqs. 2-5 can also be expressed in terms of the orbital period through Kepler's third law. In this way, for stars with convective envelopes, we have

.

$$\tau_{sync} = 3.95\times10^2\beta^2M^{7/3}\frac{(1+q)^2}{q^2}L^{-1/3}{\lambda_2}^{-1}\frac{P^4}{R^{16/3}} \qquad (15)$$

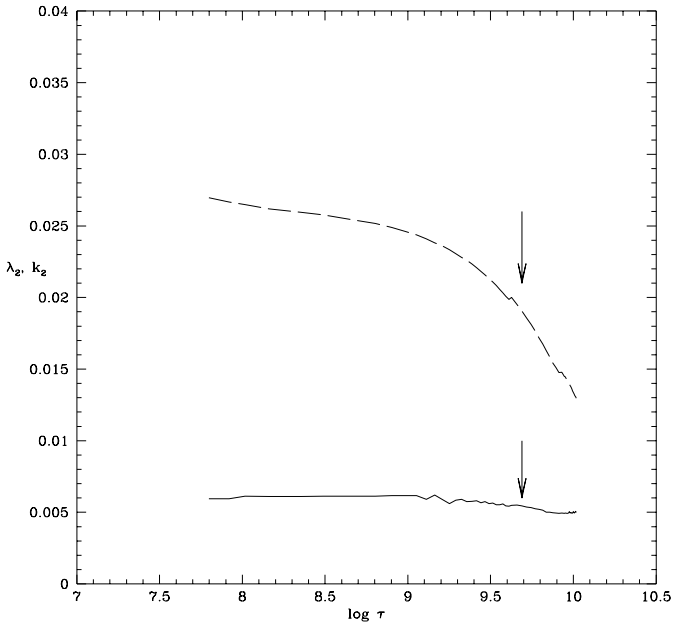

Fig. 3. The tidal coefficient λ_2 (solid line) and the apsidal motion constant k_2 (dashed) for 1.0 $M_\odot$ model during main-sequence for X=0.70 and Z=0.02. The arrows indicate the point where the central hydrogen content is reduced to about 50% of the initial value.

$$\tau_{circ} = 1.99 \times 10^3 M^3 \frac{(1+q)^{5/3}}{q} L^{-1/3} {\lambda_2}^{-1} \frac{P^{16/3}}{R^{22/3}} \qquad (16).$$

For stars with convective cores and radiative envelopes the time scales are

$$\tau_{sync} = 2.03 \beta^2 M^{7/3} \frac{(1+q)^2}{q^2} {E_2}^{-1} \frac{P^{17/3}}{R^7} \qquad (17)$$

$$\tau_{circ} = 1.71 \times 10^1 M^3 \frac{(1+q)^{5/3}}{q} {E_2}^{-1} \frac{P^7}{R^9} \qquad (18).$$

In these equations M, R and L are in solar units while P is given in days and the time scales are given in years. A few words about the coefficient λ_2: we have used Eq. 11 to compute it, i.e, we have assumed that the tidal period Π is larger than the convective turnover time. It should be also mentioned that TSC is dependent on the rotation of the stars. Therefore Eqs. 16 and 18 are valid only for nearly synchronous systems. Concerning synchronization the corresponding Eqs. 15 and 17 are valid only for small eccentricities.

Before comparing observations with theoretical predictions directly, we have simulated some hypothetical systems as we have done in the first paper of this series. For simplicity, we have assumed that the orbital period is constant during the evolution and a mass ratio equal to 1. We carried out integrations until the relative variations of eccentricity and angular velocity became 0.5 per cent of the initial value. Models starting at the ZAMS have been used. This is an important limitation and we shall return to this below.

In order to consider the contribution of both components to circularization we have used an equivalent time scale. The ordinary differential equation governing the orbital eccentricity is given by

$$-\frac{1}{e}\frac{de}{dt} = \frac{1}{\tau_{cir,1}} + \frac{1}{\tau_{cir,2}} \qquad (19)$$

where subscripts 1 and 2 denote the primary and the secondary components.

In binary stars investigations, and particularly in double-line eclipsing binaries, the surface gravity is a parameter largely used to indicate evolution. In Fig. 4 we can see the behaviour of log g_{cri} - the surface gravity for which circularization is achieved - for hypothetical systems integrating Eqs. 16 and 18. Same computations using the hydrodynamical approach are represented by dashed lines. It is easy to see that, as expected, the Zahn mechanisms are less dissipative that the hydrodynamical, for a given set of dynamical parameters. Note that, before the present computations, the values of λ_2 and E_2 were available only for a few models or for the ZAMS. We support the lower efficiency of dissipation of the Zahn mechanisms by integrating the differential equations with a proper contribution of the companion and using modern stellar models which take into account the time dependence of λ_2 and mainly of E_2.

In Fig. 5 we represent the integrated time - t_{cri} - for which circularization is achieved for the same models. The differences between the critical times using tidal and hydrodynamical mechanisms decrease with the orbital period. For a given period, the differences decrease with stellar masses. This figure can be used to compare theoretical predictions with the observed age $\times$ P(cut-off) relationship in clusters. Indeed Mathieu et al. 1992 have established that binaries with late-type components taken from different clusters present cut-off periods which are proportional to the age of the sample. Assuming that a model of 1 $M_\odot$ is representative of late-type stars in these clusters, that the period remains constant during the evolution, and that the mass ratio is 1 we can simulate the behaviour of a given cluster by integrating Eq. 19. Let us concentrate on the case when m = 1 $M_\odot$ and in the results provided by the hydrodynamical mechanism. Full hexagons denote the observed age $\times$ P(cut-off). The agreement between the observational data and the theoretical predictions can be considered as good (the ages of the clusters are only upper limits for t_{cri}) but not surprising due to the pre calibration of N and γ we performed in Paper I. Therefore the agreement obtained using the formalism by Tassoul is only a test of internal consistency but it is not conclusive.

With respect to equilibrium tide, the low efficiency of dissipation of the turbulent mechanism can be clearly seen from that figure. An artificial enhancement of the turbulent dissipation by a factor around 100-200 during the main-sequence would be sufficient to get a better fit with observed age $\times$ P(cut-off). We would like to emphasize the artificial nature of such an enhancement (see also section 4). All results presented in this paper are based on standard time scales (without enhancement) except where we have indicated explicitly the contrary. We have considered an artificial increase of the efficiency represented in

Fig. 5 by the thick line that denotes computations for a 1 $M_\odot$ model with an enhancement factor of 40. However, to justify this enhancement within the mixing-length picture, as was already pointed out by Zahn (1992) is not easy. An alternative way to conciliate theory with observational data would be the investigation of the influence of the initial conditions on the cut-off periods. Remember that the results above are valid only for little departure from the synchronism and small eccentricities. Moreover, the uncertainties in the cut-off period determination are still large (see Mathieu et al. 1992).

Also for early-type stars some interesting features can be analysed using Fig. 5. Analysing a sample of 200 early-type close binaries Giuricin et al. (1984) demonstrated that, for orbital periods above approximately 2 days, the orbits are eccentric although some circular orbits are also present beyond this critical period. The dotted line indicates this cutt-off period. Let us take the 5 $M_\odot$ as a typical early-type star. In the case of the radiative damping mechanism the observed cut-off period coincides with the end of the main-sequence, while for the hydrodynamical mechanism the intersection occurs in the middle of main-sequence. However, more recently Matthews & Mathieu 1992 established a new period-eccentricity distribution for A type binaries. The corresponding cut-off period is around 10 days. As pointed out by Matthews & Mathieu this disagreement with the work of Giurucin et al. can be due to the nature of the sample used (60 against 200 stars) or to the large range of masses in the sample of Giurucin et al. Moreover Matthews & Mathieu did not find observational evidence that the structure of the stellar envelope plays a decisive role in tidal circularization during the main-sequence.

The usefulness of the computations shown in Fig. 5 for comparison with data from close binaries systems in clusters is obvious. Due to the fact that cut-off periods in clusters are determined within spectral and chemical composition ranges, one should integrate the differential equations for several models around a mass corresponding to the typical spectral type which characterizes the binaries for each cluster. This would mean an introduction of theoretical error bars in the diagram and would possibly allow for a more realistic comparison with observations. Indeed computations based on, for example, a 0.9 $M_\odot$ model, indicate that the critical curve is shifted to higher times for a given period, while for models more massive than 1 $M_\odot$ the effect is the opposite. Of course, this method can be applied to other kind of clusters and/or to different spectral types. This is a new aspect of the investigation of the tidal evolution theories in clusters and it is certainly much more accurate than to use time scales as has been done before. We can provide, to interested readers, computations as those represented in Fig. 5 for a wide range of mass and chemical compositions.

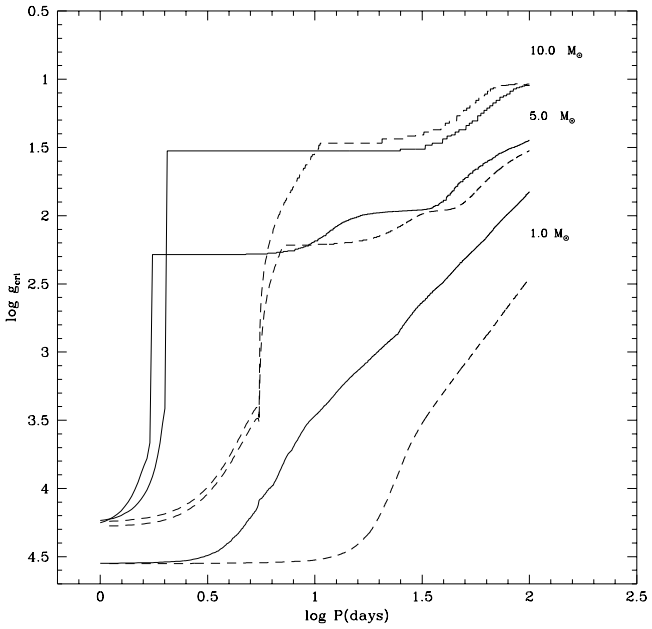

Fig. 4. Log g_{cri} for circularization for hypothetical systems with q=1. Solid lines indicate calculations using turbulent dissipation and radiative damping mechanisms and dashed ones denote those computed under hydrodynamical approach. Attached numbers indicate the masses in solar units.

3. Synchronism

The expected synchronization and circularization levels for a selected sample of eclipsing binaries with accurate absolute dimensions (Andersen 1991) were computed integrating the differential equations 15-18 through a fourth order Runge-Kutta method. All astrophysical parameters required by the set of differential equations, including evolutionary age, were obtained by comparing the theoretical models mentioned above directly for each star of the sample. We would like to emphasize that given the high dependency of the time scales on mass, and mainly on radius these kind of investigations must be performed with very accurate binary data in order to test tidal theories. In fact, Eqs. 15-18 depend on three directly observable parameters: the period, the masses and the radii. The period is one of the best known parameters in binary stars. However, the masses and radii are only well known for about 40 systems. Moreover, the sample compiled by Andersen is adequate because it contains early and late-type stars. In this way the mass range where equilibrium and dynamic tide mechanisms are expected to be active is covered. Magnetic fields, stellar winds and mass exchange are not taken into account in the present analysis.

The time scales for synchronization for late-type stars depend on $\lambda_{lm} = \lambda_2(2\pi/|l\omega - m\Omega|)$ (see Zahn 1989), where Ω and ω are the orbital and rotational frequencies respectively. The maximum value for λ_{lm} is achieved when the star is completly convective and that value depends on the selected value of the mixing-length parameter α. In the present investigation we shall assume that all λ_{lm} are equal to λ_2. That parameter was computed using Eq. 11. We think that, at the level of uncertainties of the current adopted convection theory, this is a good approximation. In fact, λ_{lm} tends to a common value when stars achieve the ZAMS (Zahn & Bouchet 1989).

In Fig. 6 we show the observed and theoretical rotational velocities at the periastron. Within uncertainties, we can consider

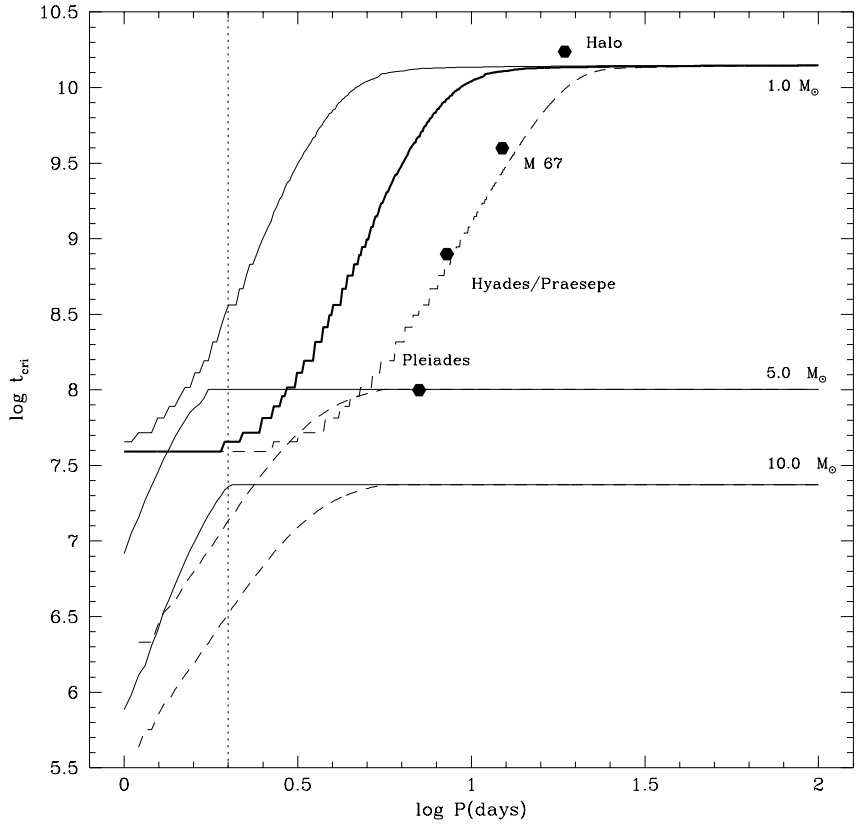

Fig. 5. Log t_{cri} for the same systems as in Fig. 4. Full hexagons represent the observed age $\times$ P(cut-off) relationship for clusters following Mathieu et al. 1992. The point corresponding to the pre main-sequence stars is not included. Dotted line denotes the cutt-off period for early-type stars. Thick line denotes the case for 1 $M_\odot$ with τ'=10^δ τ (δ=-1.6) which corresponds to an artificial enhancement by a factor of about 40.

that the stars compiled by Andersen are, on average, pseudo-synchronized. However some systems, as TZ For (discussed in another paper) and DI Her, present rotational velocities very different from the theoretical predictions. Figs. 7 and 8 show the critical times for synchronization as a function of the age of the system using the mechanisms by Zahn. These results are not incompatible with those shown in Fig. 6 since the critical times are, in most of the cases, of the order of their respectives ages. When compared with the results based on the hydrodynamical mechanism, the present critical times are, on average, more than 1 dex larger. This is an expected result given the above discussions on the efficiency of the dissipation of the different mechanisms.

It is interesting in this point to analyse the case of TZ For applying the approximation due to Zahn in order to contrast it with the results obtained in Claret & Giménez 1995a where the hydrodynamical mechanism was used. TZ Fornacis is an eclipsing binary system whose components have masses of 2.05 and 1.95 $M_\odot$ and a period of 75.7 days. The radius of the more massive component is 8.32 $R_\odot$ while the radius of the secondary is 3.96 $R_\odot$. The mean errors in masses and radii are smaller than 3 %. The primary seems to be synchronized but the secondary does not. In fact, it rotates about 10 times faster than the primary and about 16 times faster than the theoretical value. By comparing the stars with theoretical models, we infer that the primary is burning helium in the core while the secondary is near the "red hook" (see Fig. 1 by Claret & Giménez 1995a). We have integrated the differential equations which govern the eccentricity and angular velocity. The circularization and the synchronization times for the primary and for the secondary are found to be of the same order than the age. Using a very simple law for the angular momentum conservation we have scaled the rotational velocities to the ZAMS and a very satisfactory result for the present v_1/v_2 was obtained. Also, the diagnosis diagram shown in Fig. 4 (see Fig. 3 of that paper) was shown to be useful since it distinguishes the synchronous component from the asynchronous one. In this way, we have shown how both components of TZ Fornacis probably evolved, the circularization as well as the synchronization for the primary were achieved, while the secondary is still presenting high degree of asynchronism.

The components of TZ Fornacis presented radiative outer layers and a convective core during the main-sequence but at the present stage they have convective envelopes. This means that the main braking mechanism was changed from radiative damping to turbulent dissipation. This makes it an excellent example to compare with the two possibilities embraced by Zahn's investigations. We have performed that test. Fig. 9 shows the evolution of the two components of TZ Fornacis in the log R-log age diagram. A common age of 1.3 Gyears (log age around 9.1) seems to be adequate to describe the system. By integrating Eq. 19 and its corresponding equation for synchronization using the time scales given by Eqs. 15-18 (for i=1,2) we have found log t_{sinc1}=9.05, t_{sinc2}=9.13 and t_{cir}=9.05. By inspecting Fig. 9 we can conclude, within the observational and theoretical uncertainties, that the circularization of the orbit and the

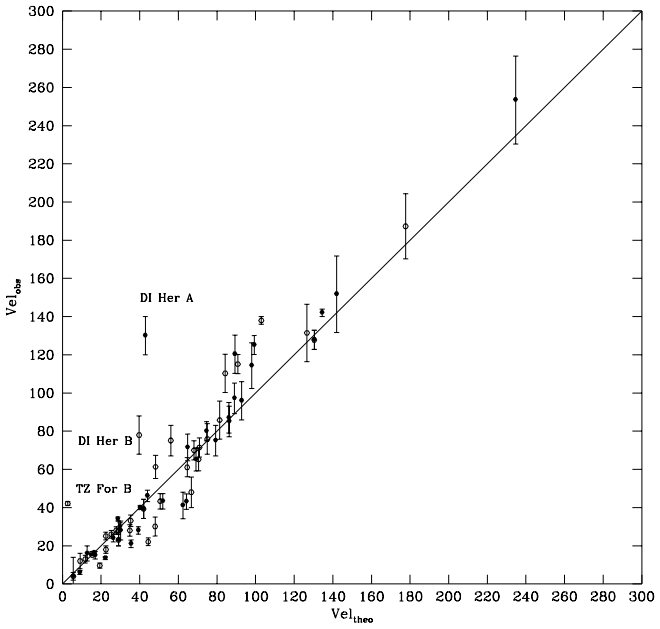

Fig. 6. Observed and theoretical rotational velocities assuming synchronization at periastron. Full hexagons denote primaries and open ones represent the secondaries. Note the position of the components of DI Her and TZ For B.

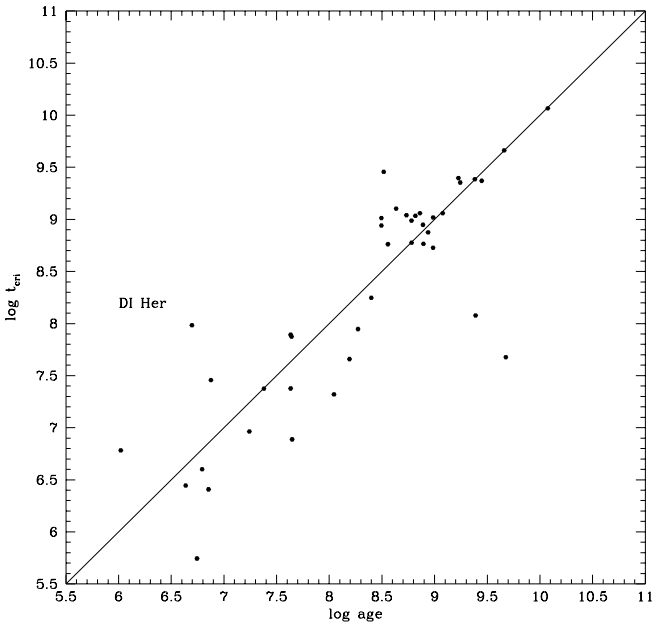

Fig. 7. Critical times for synchronization using the turbulent dissipation and radiative damping mechanisms versus the age. Case of primaries. The position of DI Her is indicated.

synchronization of the more massive star should occur almost simultaneously, corresponding to the local maximum of radius of the primary component. Similarly, synchronization for the secondary should occur at log age=9.13, which also coincides with a local maximum for the radius of the secondary component. Both formalisms seem to be capable to explain the observational constraint but inspection of Fig. 5 reveals that for large periods we find an asymptotic behaviour for a given system. These systems tend to circularize the orbits when they are in or beyond the giant branch. This is just the case of TZ For. The small differences between the critical times for synchronization for both components of this system can be attributed to the large changes in the momenta of inertia in small time intervals.

4. The levels of circularization

Synchronization levels do not give as conclusive results as in the case of the circularization of orbits: while for the latter case we can say if a system is eccentric or not, a similar reasoning can not be applied directly to synchronization, since the interior can rotate at a different angular velocity than the envelope does. Before beginning to analyse the levels of circularization of our sample, a few words of caution: as we do not know a priori what are the initial eccentricity and rotational velocities, the hypothesis of decay to 0.5% of their initial values to characterize the critical times may be arbitrary from the observational point of view. In fact, systems with smaller initial eccentricities would need less time to achieve critical points - the eccentricities are no longer detected observationally - when compared with more eccentric systems.

The evaluation of the levels of circularization of the stars in the sample are based on the integration of Eq. 19 using Eqs. 16 and 18 as time scales for early and late-type stars respectively. We have assumed that the period remains constant during the star lifetime. We have plotted in Fig. 10 the observed eccentricities versus log (t/t$_{cri}$) where t is the age of the system. The results are satisfactory, especially for the more eccentric orbits, since all these systems are on the left of the zero point, i.e., their ages are smaller, and in some systems equal, to their predicted circularization times.

A comparison with the results based on the hydrodynamical approach shows that the behaviour of eccentric systems is similar, with one remark: due to the high dissipation of the hydrodynamical mechanism, more systems are found on the right side of the diagram than in the case of Zahn mechanisms. If on the one hand the hydrodynamical mechanism "explains better" the circular orbits, on the other hand some eccentric systems are found with ages greater than their respective circularization times. This intercomparison is based on the factor γ which was introduced by Tassoul (1988) and "calibrated" by us in Paper I using the same sample of eclipsing binaries. The introduction of such a factor is being strongly discussed (Zahn 1996). In order to see how the hydrodynamical mechanism with γ=0 compares with the observations, we present in Fig. 11 the results of such calculations. As one can see in that figure, the efficiency of the hydrodynamical mechanism increases too much and it is capable of explaining only the systems with circular orbits.

We have artificially increased the efficiency of the tidal-torque and resonant mechanisms by introducing a constant in Eqs. 16-18 **only to estimate** the magnitude of the discrepancy

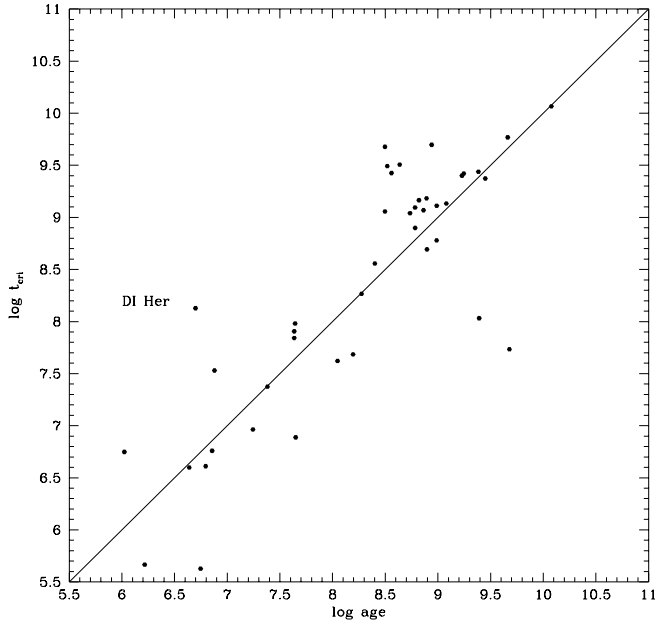

Fig. 8. Same remarks as in Fig. 7. Case of the secondaries. The position of DI Her is indicated.

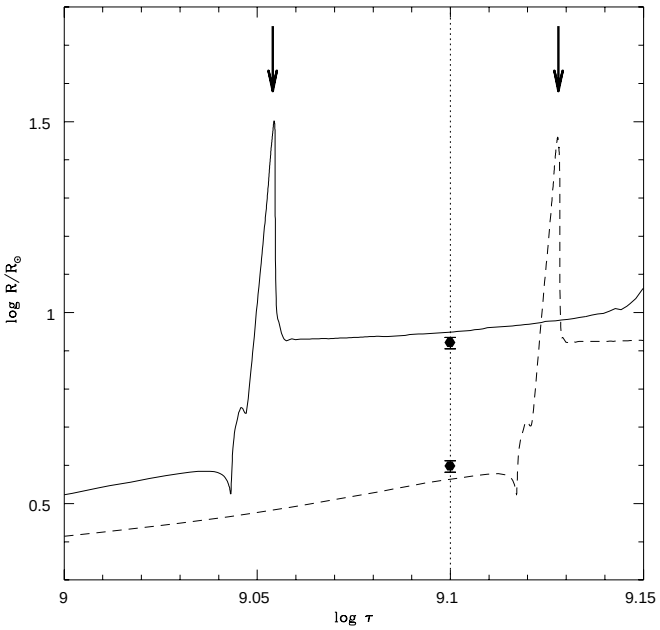

Fig. 9. The evolution of the radii of TZ For. The continuous line represents the primary while the dashed one denotes the secondary. The left side arrow indicates the point where circularization and synchronization of the primary are achieved. The other arrow indicates the time where the secondary would synchronize.

between theory and observation. As expected, the new time scale τ' where $\tau' = 10^{\delta}\tau$ and δ=-1.6, changes the general results in such a way that the comparison with the observed age $\times$ period(cut-off) relationship for clusters is improved (Fig. 5). Taking into account these enhanced time scales and integrating the differential equation for our sample of binaries, the largest corrections, with respect to the results presented in Fig. 10, have been found for the systems with smaller eccentricities and periods.

An alternative way to see how the theoretical levels of circularization compare with observational data is to plot log (g_{cri}/ g_{obs}) versus eccentricities. Fig. 12 shows the results for the present integrations (there is an error in the horizontal label of Fig. 6 of Paper I. The label should be changed to log g_{cri} - log g_{obs}). Figs. 10 and 12 are very important in spite of the circularization theory used since they include the observed masses, radii, periods, eccentricities, evolutionary models and tidal evolution theories through log t_{cri} and log g_{cri}.

5. Concluding remarks

To decide which mechanism is the best to describe the orbital evolution of close binary systems is not a simple task given the uncertainties in the theories of the braking mechanisms, including the discussion of the validity or not of the hydrodynamical approach. However, regardless of the dissipation mechanism used, we would like to stress the fact that the differential equations which govern the orbital parameters of a binary system must be **integrated** instead of using the corresponding time scales. Moreover, we have assumed several approximations in this investigation: constant periods during the integration of the differential equations, little departure from synchronism, small eccentricities, etc. As pointed out by Zahn (1989, 1992) the integration of the differential equations which control the orbital parameters depends strongly upon the initial conditions. Besides the limitations and approximations quoted above, the most crucial limitation was probably not to consider the pre main-sequence evolution. This important phase shall be taken into account in a future work.

Apart from the validity or not of the formalism by Tassoul (for a detailed discussion see Rieutord 1992 and Tassoul & Tassoul 1996), the results obtained using this mechanism (Paper I) depend upon the calibration of the free parameters N_r, N_{conv} and γ. We have found that the value of γ that provides the best fitting with observations is 1.6, i.e, with this value the efficiency of the mentioned process was reduced about 40 times. This reduction could be justified following Tassoul & Tassoul 1996 due to the fact that the effects of non-linearity and baroclinicity were not adequately considered. The highly eccentric systems are found to be on the left side of the zero point of the e $\times$ log (t/t_{cir}) diagram, while the circular orbits are found to be on the right side. Concerning synchronization, the critical times are smaller, or of the same order, as the ages of the systems. This is in agreement with observations of pseudo-synchronization in close binary systems. However, the agreement between the theoretical predictions using the hydrodynamical mechanism with the observed age $\times$ Period (cut-off) should be taken only as an internal consistency test, because N and γ were pre calibrated using Andersen's list of binaries in Paper I.

The theoretical predictions by Zahn seem to be in agreement with the eccentricity distribution of our sample of binary

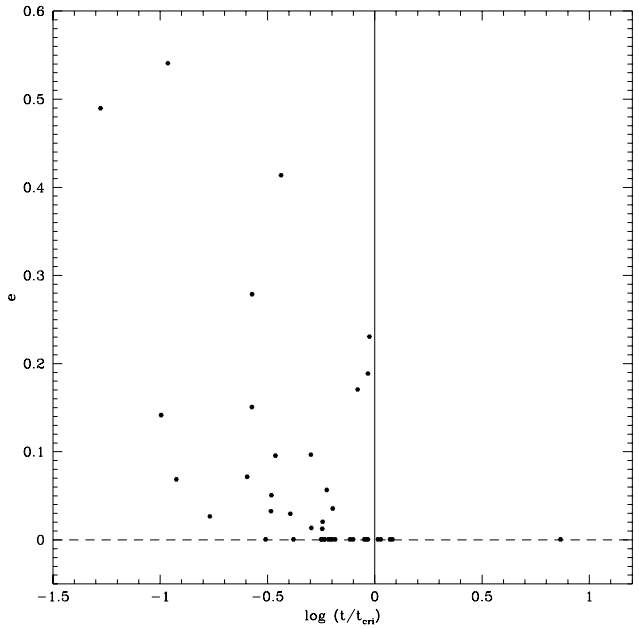

Fig. 10. Comparison between the evolutionary ages and critical times for circularization using turbulent dissipation and radiative damping mechanisms.

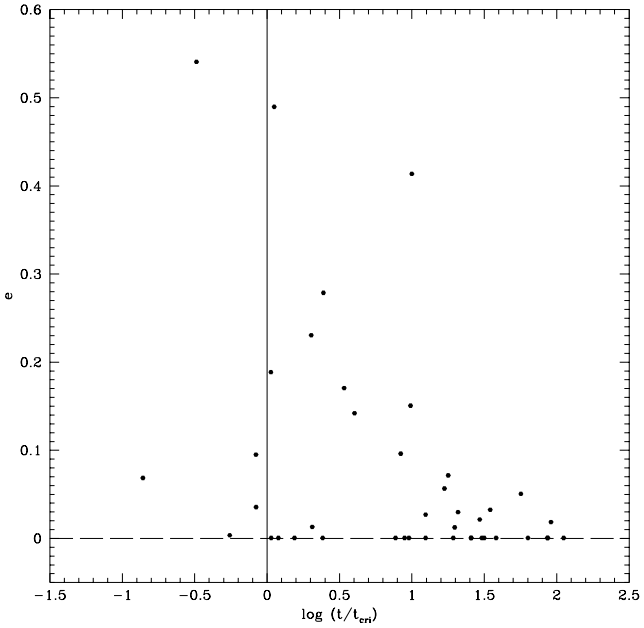

Fig. 11. The same as for Fig. 10 but using the hydrodynamical mechanism. The time scale for circularization was taken as the spin-down time (γ=0). Note the different scale in the horizontal axis with respect to Fig. 10.

stars although they can not explain some systems with circular orbits that present ages smaller that their respectives critical times. Could these systems circularize their orbits during the pre main-sequence phase? Could they be systems with zero initial eccentricities? These questions are very hard to answer at the actual level of knowledge of tidal theories.

The interesting case of TZ For can be explained by the hydrodynamical mechanism (Claret & Giménez 1995a) and by the formalism of Zahn (this paper) without the introduction of an artificial enhancement. This fact can be explained by the asymptotic behaviour of the critical times when the periods become large. Due to this, this interesting case of asynchronism can not be used as a secure test for the current tidal evolution theories.

In order to compare the theoretical predictions with the observed age $\times$ Period(cut-off) relationship we have integrated the differential equation which governs the eccentricity for a specific mass range (in this case, stars with convective envelopes). The resulting diagram $t_{cri} \times$Period can easily be used to test the validity of a given dissipation mechanism. This method supersedes the evaluation of theoretical cut-off periods based on time scales only. We have found that the turbulent friction mechanism is not dissipative enough to fit the observations of the age $\times$ Period(cut-off) relationship by Mathieu et al. 1992. An investigation on the influence of the initial orbital elements on the cut-off periods is needed in order to get more accurate conclusions. In fact, as an example, if we take 10% as a typical error in the mass of the 1 $M_\odot$ model presented in Fig. 5, a variation of almost 1 day is found in the cut-off period.

The situation of the tidal evolution theory is not clear nowadays in the light of the above discussion and of the new observational data. The question of the validity of the Tassoul

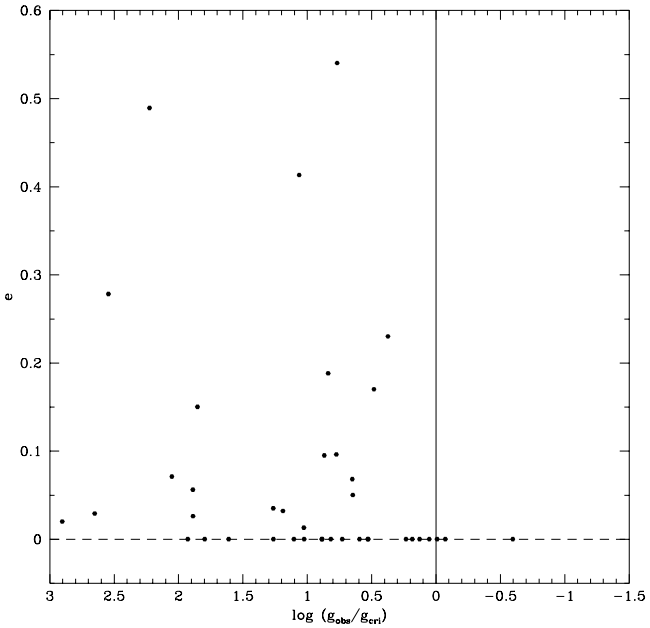

Fig. 12. Comparison between the observed surface gravity and critical values for circularization. Same remarks as for Fig. 10.

mechanism is not yet clarified. On the other hand Zahn's mechanisms are not dissipative enough to explain some systems with circular orbits and the observed age×Period(cut-off) for clusters. We think that investigations on the levels of circularization of pre main-sequence close binaries could bring to light new interesting aspects of the tidal evolution theory.

Acknowledgements. Thanks to Drs. J. P. Zahn for calling our attention on the paper by Dr. Rieutord and for helpful correspondence as well as to Dr. J. L. Tassoul for useful discussions. We acknowledge the support for the development of the present work that has been received from the Spanish DGICYT through projects PB92-0731 and PB93-0134. Financial support has also been received from the Brazilian Agency CAPES (N.C.S.Cunha proc. 2086/91-06). We thank Drs. M. A. Lopez-Valverde and V. Brown for careful reading of the manuscript and correction of the English.

References

Alexander, D.R. 1992, private communication
Andersen, J. 1991, A&AR, 3, 91
Claret, A. 1995, A&AS, 109, 441
Claret, A. 1996, submitted to A&AS
Claret, A. 1995c, in preparation
Claret, A., Giménez, A. 1993a, A&A, 277, 487
Claret, A., Giménez 1993b, in Inside the Stars, (IAU Symp. 137), eds. W. W. Weiss, A. Baglin, PASPC, 469
Claret, A., Giménez, A. 1995a, A&A, 296, 180
Claret, A., Giménez, A. 1995b, A&AS, 114, 549
Claret, A., Giménez, A., Cunha, N. C. S. 1995, A&A, 299, 724 (Paper I)
Giuricin, G., Mardirossian, Mezzetti, M. 1984 A&A, 134, 365
Huebner, W. F., Merts, A. L., Magge, N. H., Argo, M.F. 1977, Los Alamos Scientific Laboratory Report, LA-6760-M
Iglesias, C. A., Rogers, F. J., Wilson, B. G. 1992, Ap. J., 397, 771
Kopal, Z. 1989, The Roche Problem, Kluwer Academic Press, Dordrecht
Mathieu, R. D., Duquennoy, A., Latham, W. L., Mayor, M., Mazeh, T., Mermilliod, J. C. 1992 , in Binaries as tracers of stellar formation, A. Duquennoy and M. Mayor (eds), Cambridge University Press, 278
Matthews, L. D., Mathieu, R. D. 1992 , in Complementary approaches to double and multiple star reasearch, H. A. Mcalister and W. I. Harkopf (eds), ASP Conference Series, vol. 32, 244
Mayor, M, Mermilliod, J. C. 1984, in Observational tests of the stellar evolution theory, A. Maeder and A. Renzini (eds), D. Reidel Publ. Co., Dordretch, 411
Nieuwenhuijzen, H., de Jager, C. 1990 A&A, 231, 134
Reimers, D. 1977, A&A, 61, 217
Rieutord, M. 1992, A&A, 259, 581
Tassoul, J. L. 1987, ApJ, 322, 856
Tassoul, J. L. 1988, ApJ, 324, L71
Tassoul, J. L., Tassoul, M. 1996, Fundamentals of Cosmic Physics, in press
Tassoul, M., Tassoul, J. L. 1992, ApJ, 395, 604
Zahn, J. P. 1966, Ann. Astrophys., 29, 489
Zahn, J. P. 1970, A&A, 4, 452
Zahn, J. P. 1975, A&A, 41, 329
Zahn, J. P. 1977, A&A, 57, 383
Zahn, J. P. 1996, private communication
Zahn, J. P. 1984, in Observational tests of the stellar evolution theory, A. Maeder and A. Renzini (eds), D. Reidel Publ. Co., Dordretch, 379
Zahn, J. P. 1989, A&A, 220, 112
Zahn, J. P. 1992, in Binaries as tracers of stellar formation, A. Duquennoy and M. Mayor (eds), Cambridge University Press, 253
Zahn, J. P., Bouchet, L. 1989, A&A, 223, 112

This article was processed by the author using Springer-Verlag LaTeX A&A style file *L-AA* version 3.